Long-Term Variation of the Interplanetary H Lyα Glow: Voyager UVS Measurements and Implications for the Solar H Lyα Irradiance

Giuliana de Toma, Eric Quémerais, Bill R. Sandel

HAL Id: insu-02902249
https://insu.hal.science/insu-02902249

Submitted on 18 Jul 2020

LONG-TERM VARIATION OF THE INTERPLANETARY H Lyα GLOW: *VOYAGER* UVS MEASUREMENTS AND IMPLICATIONS FOR THE SOLAR H Lyα IRRADIANCE

GIULIANA DE TOMA

High Altitude Observatory, National Center for Atmospheric Research, Boulder, CO 80307

ERIC QUÉMERAIS

Service d'Aéronomie du CNRS, 91371 Verríeres le Buisson, France

AND

BILL R. SANDEL

Lunar and Planetary Laboratory, University of Arizona, Tucson, AZ 85721

ABSTRACT

In this paper we study interplanetary (IP) Lyα data taken with the *Voyager 1* and *Voyager 2* spacecraft from 1980 to 1995. The coverage in time is equal to about 156 and 220 points yr^{-1} for *Voyager 1* and *Voyager 2*, respectively, with almost no gaps. The IP Lyα data are normalized for spatial changes in the emissivity, which arise from variations in observing geometry, by using a radiative transfer model. The normalized data show the variation of the solar H Lyα line-center flux during the solar cycle. We compare this variation with the solar H Lyα irradiance measurements of integrated flux from the *Solar Mesosphere Explorer* and the *Upper Atmosphere Research Satellite*/Solar-Stellar Irradiance Comparison Experiment (SOLSTICE), and, when direct solar measurements are not available, we use estimated irradiances from magnesium and helium indices. The comparison between *Voyager* IP data and solar data shows that the best agreement is found with the SOLSTICE set of measurements, when no differences in the variation of the line-center flux and the integrated flux are taken into account.

Subject headings: interplanetary medium — Sun: fundamental parameters — Sun: UV radiation

1. INTRODUCTION

The interplanetary (IP) Lyα glow emission, which results from resonance scattering of solar Lyα photons by neutral hydrogen atoms in the interplanetary medium, has been known for more than 25 years (Bertaux & Blamont 1971; Thomas & Krassa 1971). During this time, a number of spacecraft experiments have studied the IP Lyα emission. Earlier analyses of these data concentrated on the character of the interstellar cloud of hydrogen surrounding the Sun. Later work also included investigations of the solar H Lyα flux and of the solar wind. A list of the various data sets is found in Ajello et al. (1987) and Quémerais et al. (1994). The long duration of some planetary missions offers the opportunity for long-term studies of the IP H Lyα emission. For example, Shemansky, Judge, & Jessen (1984) and Quémerais, Sandel, & de Toma (1996) used the variation of IP emission correlated with the solar rotation period to estimate the neutral hydrogen density, and Ajello et al. (1987) used *Pioneer Venus* UVS measurements to track the emission over about one-half of a solar cycle, from 1979 through early 1985.

In this paper we present the Lyα observations collected with the Ultraviolet Spectrometers (UVS) on the *Voyager 1* and *2* spacecraft between 1980 and 1995. These two large data sets, which span more than one solar cycle, provide a unique opportunity to study the relationship between the solar Lyα variation during the solar cycle and the corresponding variation of the H Lyα seen as IP emission. The data consist of sky background observations with long integration times that clearly show an IP Lyα signature. The data have good coverage in time, but different data points usually have different pointing directions. Therefore, before a direct comparison with solar data can be made, the sky background data must be corrected for spatial variations in emissivity induced by the distribution of hydrogen in the interplanetary medium. For this purpose, it is necessary to know the distribution of hydrogen in the heliosphere and to have a model that realistically describes the multiple scattering effects. We have used the radiative transfer model computation of Quémerais & Bertaux (1993). The model has the advantage, over an optically thin approximation, of taking into account the damping caused by multiple scattering of the solar Lyα from the IP medium as well as the corresponding increase in local emissivity due to photons with a high order of scattering. This effect, which is almost negligible at 1 AU, becomes important at the present position of the two spacecraft in the outer solar system (Keller, Richter, & Thomas 1981). To make the computation more feasible, some simplifying assumptions have been used in the model. We do not consider the interaction of the expanding solar wind with the interstellar plasma, which may cause an increase in the hydrogen number density in the upwind direction (Quémerais et al. 1995). Consequently, data points in the region of possible enhanced density have been omitted from our analysis.

The aim of this paper is to compare observations of solar Lyα irradiance with *Voyager* IP Lyα data as they vary with solar activity and to analyze how the fit between the two time series changes with the solar and interstellar parameters used in the model computations. The comparison of solar and IP Lyα is hampered by the fact that IP Lyα emission depends only on the intensity at the line center, while solar observations measure the integrated line flux. At present, a well-established relation between the H Lyα integrated line flux and the line-center flux does not exist. Because the *Voyager* data give a good estimate of the rela-

tive minimum-to-maximum ratio during the solar cycle, different hypotheses can be tested against *Voyager* data to improve our understanding of solar Lyα variability. On the other hand, it is difficult to derive absolute solar irradiances for the above reasons and because of uncertainties in the *Voyager* UVS calibration at Lyα. This is particularly unfortunate, since the more recent solar measurements indicate higher values for solar Lyα irradiance, which imply a larger value for the ratio of the solar radiative pressure to the gravitational force. This is important for models of the IP medium and will lead to a very different description of the region in the vicinity of the Sun, if these higher irradiances are confirmed by future observations.

Finally, it is important to point out that the *Voyager* data sets represent the longest set of periodic observations of the Lyα background and so of the solar Lyα flux at line center. These data are very important for other space experiments, such as the Solar Wind ANisotropies (SWAN) on the newly launched *Solar and Heliospheric Observatory (SOHO)* mission (Bertaux et al. 1995), which is studying the IP hydrogen distribution and needs solar Lyα irradiance information to interpret the measurements.

2. INSTRUMENT AND DATA ANALYSIS

We analyze the IP Lyα observations made by the UVS on the *Voyager 1* and *2* spacecraft over more than 15 years, from 1980 to 1995, covering more than one solar cycle. During these years the two spacecraft have explored a large region of the planetary system as shown in Figure 1 and Table 1. *Voyager 1* left the ecliptic plane after its Saturn encounter in 1980. In 1995, it was at a distance of 60 AU from the Sun and at a latitude about 34° north of the ecliptic plane. *Voyager 2* traveled near the ecliptic plane until its Neptune encounter in 1989. In 1995, it was at a distance of 46 AU from the Sun and at a latitude of about 18° south of

TABLE 1
LOCATION DATA FOR *Voyager 1* AND *Voyager 2*

Parameter	1980	1985	1990	1995
Voyager 1				
d (AU)	8.3	23.6	41.7	59.9
b_{ecl} (deg)	2.2	29.2	32.9	34.0
a_{upw} (deg)	79.4	31.9	27.7	27.1
Voyager 2				
d (AU)	7.0	17.4	32.3	46.2
b_{ecl} (deg)	0.1	−1.0	−2.9	−17.7
a_{upw} (deg)	84.1	7.4	29.3	39.3

NOTE.—Parameters are distance from the Sun (d), inclination on the ecliptic plane (b_{ecl}), and angle with the direction of the interstellar neutral hydrogen flow (a_{upw}).

the ecliptic plane. The positions of the two spacecraft, relative to the flow of hydrogen entering the solar system from the local IS medium, are in the upwind direction. The angles between the flow direction and the line from the Sun to the spacecraft are ~27° for *Voyager 1* and ~39° for *Voyager 2*.

The two UVS instruments, which are identical except for a small shift in wavelengths, have been described extensively in the previous literature (Broadfoot et al. 1977; Broadfoot & Sandel 1977), and only a brief presentation is given here. They are compact Wadsworth objective grating spectrometers located on a scan platform that can rotate about two axes. A mechanical collimator defines the field of view to be 0°.10 FWHM × 0°.87. The photon-counting detector consists of a dual microchannel plate (MCP) electron multiplier and a linear readout array of 128 channels. They operate in the wavelength region from 50 to 170 nm with a spectral resolution of about 3.3 nm for extended sources.

The two UVS instruments have been very consistent and stable throughout the years, as shown by the large number of stellar observations made during the *Voyager* mission. Spectra of reference stars, used for monitoring in-flight calibration, show less than 5%–6% change in the instrument response after 1980, but the absolute photometric calibration is less accurate at H Lyα and is not applied to the data presented here.

The two UVS instruments have collected data continuously since 1977, including many observations of dark regions of the sky without stellar or planetary targets. These observations show a clear signature of solar Lyα resonantly scattered by hydrogen atoms in the IP medium. The intensity of the line decreases with the distance from the Sun, but it remains easily measurable even at the present distances of the spacecraft.

The IP Lyα observations analyzed here were sometimes made to study the IP medium or to obtain the sky background close to an astrophysical target of interest, but they could also occur during normal spacecraft operations. Therefore, these observations were not taken in a regular way. There is usually a good coverage in time, except for a few gaps, but the data represent lines of sight in very different directions. The histogram in Figure 2 shows the distribution of the observations for both spacecraft between 1980 and 1995 in 3 month bins. Data are available at an average of 156 observations yr^{-1} with *Voyager 1* and 220 observations yr^{-1} with *Voyager 2* for a total of 2416 and 3419 observations, respectively. There is usually better coverage in time for *Voyager 2*; in particular, the years
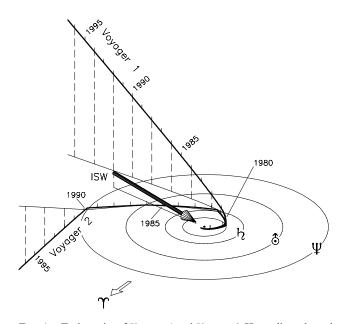

FIG. 1.—Trajectories of *Voyager 1* and *Voyager 2*. Heavy lines show the trajectories, and lighter lines show their projections onto the ecliptic plane. The orbits of the outer planets, Jupiter, Saturn, Uranus, and Neptune, are also shown. *Voyager 1* turned north of the ecliptic plane at Saturn encounter, while *Voyager 2* turned south at Neptune. The motion of the interplanetary medium relative to the Sun is shown by the large arrow marked "ISW." Its projection onto the ecliptic plane is shown below it. The small arrow is in the direction of the vernal equinox.
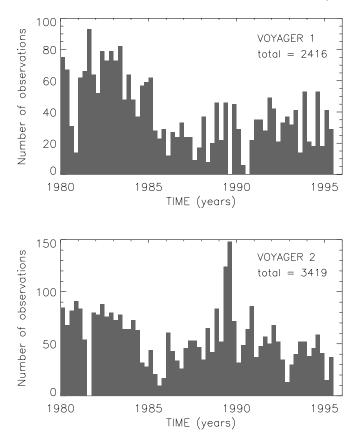
FIG. 2.—Distribution of *Voyager 1* and *Voyager 2* IP Lyα measurements from 1980 to 1995 with a 3 month bin. The observations close to the Sun or to the ecliptic poles have been omitted. During the later years, observations near the upwind direction have also been omitted. Both spacecraft show good coverage in time with usually more observations with *Voyager 2* than with *Voyager 1*. Only three periods without data are visible: in 1989 and 1990 for *Voyager 1* and in 1981 for *Voyager 2*.

between 1989 and 1991, which correspond to the solar maximum of cycle 22, are well represented by *Voyager 2* measurements with only a few irregular observations for *Voyager 1*.

For sky background observations, the integration time for a single spectrum is generally 3.84 or 240 s. All the spectra in a time period of 24 hr, with pointing direction inside a region of the sky 10° wide in right ascension and declination, are added together to produce daily values. A minimum of 3 hr total integration time is required to ensure good counting statistics. To eliminate stellar spectra or scattered diffuse starlight in the final product, a test for the presence of stars is performed before adding the spectra. A second test for stellar contamination is performed on the summed spectra by comparing the wavelength regions between 98 and 105 nm (hot stars) and 134 and 142 nm (cooler stars) to the Lyα region. All spectra with an average count rate higher than 0.05 counts s^{-1} or exceeding 5% of the Lyα intensity in these special wavelength regions are rejected. These procedures ensure that the final data are free from contamination caused by stars or other astrophysical objects.

Scattering of sunlight into the instrument is potentially troublesome. When the Sun illuminates the entrance aperture, some of the sunlight may be scattered by the front collimator plate and enter the instrument. Experience has shown that significant scattering may be present when the line of sight is within about 8° of the Sun. To avoid contamination by sunlight, we have omitted observations made within 20° of the Sun.

The radiative transfer models of the IP medium used here assume a homogeneous hydrogen distribution at large distances, and they do not include the interaction of the solar wind with the interstellar plasma at the heliopause and the consequent increase of the hydrogen density in the direction of the incoming wind (Osterbart & Fahr 1992; Baranov & Malama 1993). Therefore, we have omitted the observations within 50° of the upwind direction after the year 1990 for *Voyager 1* and 1992 for *Voyager 2*, which are times when the influence of increasing hydrogen density would potentially affect the observed Lyα intensity. As a matter of fact, all the observations in the upwind direction show a trend toward higher values when compared to other directions. This effect is consistent with other studies of *Voyager* data and was discovered in *Voyager* observations in 1993 (Hall et al. 1993; Quémerais et al. 1995).

The observations presented have been reduced using the standard analysis procedures for *Voyager* observations (Holberg & Watkins 1992) to correct for instrumental effects, but no absolute calibration is applied. The channel-to-channel variations in the sensitivity of the detector are corrected, scattered light is removed, and the background signal (mainly γ-rays from the radioisotope thermoelectric generator on board the spacecraft and cosmic rays) is subtracted. The error in the final spectra associated with the data reduction process is difficult to estimate. Assuming that the behavior of the instruments has not changed appreciably through time, the first correction should be quite accurate, but the removal of scattered light with high accuracy is difficult. The background subtraction is not a significant source of error in the early years, when the IP Lyα is strong compared to the background, but it becomes more important in recent years, when the IP Lyα line is weaker. The accuracy of the background removal is tested on the continuum shortward and longward of the Lyα. Spectra for which the error in the background subtraction is estimated to exceed 5% of the Lyα intensity are rejected.

3. SOLAR Lyα IRRADIANCE

Other than a few rocket flights (Mount & Rottman 1983a, 1983b, 1985; Woods & Rottman 1990), only two major satellite missions have measured solar integrated Lyα irradiances in the last 15 years: the *Solar Mesosphere Explorer* (*SME*) from 1981 October to 1989 April (White, Rottman, & Livingston 1990) and the *Upper Atmosphere Research Satellite* (*UARS*) launched in 1991 September and still operating. *UARS* carries two solar instruments able to measure Lyα irradiance: the Solar-Stellar Irradiance Comparison Experiment (SOLSTICE) (Rottman, Woods, & Sparn 1993; Woods, Rottman, & Ucker 1993) and the Solar Ultraviolet Spectral Irradiance Monitor (SUSIM) (Brueckner et al. 1993).

In this work we use both *SME* and *UARS*/SOLSTICE measurements of solar Lyα irradiance. Although the *UARS*/SUSIM Lyα measurements are not used, they are consistent with the SOLSTICE Lyα values, with which they agree within 10% (Woods et al. 1996).

The *SME* satellite operated in the years 1981–1989, monitoring the declining phase of solar cycle 21 and the rising phase of solar cycle 22. Its prelaunch photometric calibration was traceable to photodiodes calibrated by the

National Institute of Standards and Technology (NIST, formerly NBS). While in orbit, *SME* was calibrated by a series of seven sounding rocket flights (Mount & Rottman 1983a, 1983b, 1985) launched between 1982 and 1986. *SME* incorporated two redundant sets of scattering screens to direct solar radiation into the spectrometer. One surface was used daily, and the second was preserved and used infrequently, every 2 or 3 months, to serve as a more reliable reference surface. The *SME* mission was intended for a duration of only 1 year, and the primary science objective of the solar instrument was to record short- to intermediate-term solar variability lasting on the order of 1–2 months. This experiment was not equipped to track the instrument response over longer time periods, and although the sounding rocket measurements were available, they provided a calibration transfer accurate only to ±10%. Moreover the rocket calibrations were discontinued after 1986 March, leaving no reliable calibration during the rise of solar activity into solar cycle 22. There is a relative uncertainty in the *SME* Lyα data set increasing at about ±1% yr^{-1}, which implies that the ratio of a value obtained in 1989 to an initial value in 1982 is known to about ±10%.

SOLSTICE began its solar observations in 1991 October toward the end of the maximum period of solar cycle 22 and has been operating continuously since then. Preflight calibrations of SOLSTICE were made at NIST. At the Lyα wavelength, both photodiodes and synchrotron radiation from the Synchrotron Ultraviolet Radiation Facility II (SURF II) were used (Woods et al. 1993). In flight the sensitivity is monitored by observing bright early-type stars that are known to be stable at UV wavelengths. The stellar observations are made routinely during the night portion of the satellite orbit and provide a reliable method to track and correct the degradation of the instrument to a 1%–2% level of accuracy.

Lyα measurements from *SME* and *UARS*/SOLSTICE are shown in the top panel of Figure 3. The two missions do not overlap in time, which makes a direct comparison impossible, but, on the basis of solar observations at other wavelengths, we would expect a similar behavior of Lyα during the two solar cycles. The two sets of Lyα irradiance measurements differ instead in absolute values and variability. If we neglect the 27 day rotational modulation and consider only the long-term variability, we find that, for solar cycle 21, *SME* data show an average Lyα irradiance at solar minimum of about 2.5×10^{11} photons cm^{-2} s^{-1} and a value of about 4.0×10^{11} photons cm^{-2} s^{-1} for solar maximum. This last value is only an estimate because *SME* was not operating during the period of higher solar activity in 1981. This range corresponds to a total variability of 60%. SOLSTICE data indicate, for solar cycle 22, an average maximum value of 6.0×10^{11} photons cm^{-2} s^{-1} and a value of 3.5×10^{11} photons cm^{-2} s^{-1} in 1995, with a total variability of 70%. The year 1995 was a period of low solar magnetic activity, but not yet at solar minimum, so the total variability over the solar cycle as seen by SOLSTICE is actually higher. The SOLSTICE values appear incompatible with those of *SME*, especially for periods of high magnetic activity of the Sun. It is unlikely that the Sun was so different during the two cycles because observations at different wavelengths, e.g., the He I 1083 nm, the Mg II lines, the Ca II lines, and the radio flux at 10.7 cm (Harvey et al. 1997), do not suggest such a difference but, rather, show that the last two solar cycles were quite similar. These other
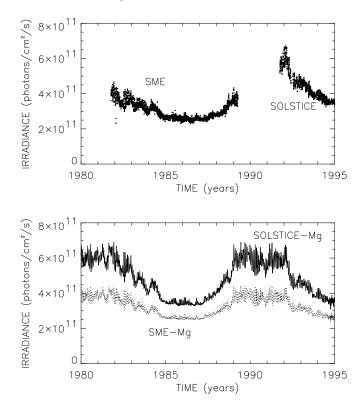

FIG. 3.—*Top*: Measurements of the integrated solar H Lyα line made by *SME* and SOLSTICE. *Bottom*: Solar H Lyα irradiance estimated from the Mg II index using a linear relationship with the *SME* and SOLSTICE data that separate the long- and short-term variability. Notice the difference, both in absolute intensity and variability, between the SOLSTICE and *SME* Lyα irradiances.

emissions originate in a region of the solar atmosphere close to the Lyα formation region and are usually highly correlated with Lyα irradiance. Therefore, it seems more likely that the difference between *SME* and SOLSTICE data is related to differences in the absolute photometric calibration of the instruments and/or a possible error in the degradation corrections applied in-flight. At present, it may not be possible to determine which values, *SME* or SOLSTICE, better represent the Lyα irradiance. Nevertheless, the extremely accurate calibration of the SOLSTICE and the validation of an independent instrument like SUSIM strongly suggest that the SOLSTICE Lyα values are more reliable (Woods & Rottman 1997). These higher solar fluxes have consequences for the models of the IP medium, for they imply a larger ionization cavity around the Sun, which seems incompatible with photometric measurements of the IP Lyα glow pattern measured by *Prognoz* (Bertaux et al. 1985), *Galileo* (Pryor et al. 1992; Ajello et al. 1994), or the early observations from the *Voyager* UVS (Lallement et al. 1991). We do not discuss this problem because, at the distances of the two *Voyager* spacecraft, models are not particularly sensitive to the hydrogen distribution near the Sun. Moreover, because the two spacecraft are moving toward the upwind direction, the size and shape of the downwind photoionization cavity is not very important for the majority of the *Voyager* observations.

Because of their differences, we do not attempt to combine *SME* and SOLSTICE data. We compare *Voyager* data with each one separately, and we use indices of solar activity (Lean 1988) to derive Lyα fluxes and extend them

backward or forward in time during years of no data. To estimate Lyα, we choose the Kitt Peak He I line 1083 nm equivalent width (Harvey 1981) and the NOAA Mg II core-to-wing ratio (Donnelly 1991). These indices have the advantage of an extended time coverage of measurements (helium has been measured since 1974 and magnesium since 1978) and a high linear correlation with Lyα data (typical linear correlation coefficients of 0.95 or higher). The good correlation between Lyα and proxy data is mainly caused by the similar long-term trend in the data sets, but nonlinearities are also present. Besides, estimated solar fluxes have a larger error when extrapolated several years beyond the actual data used to derive the linear relationships.

We found that the Mg II index gives a better representation of Lyα than the He I index, and we rely on it mainly in our analysis. We tried a simple linear relation between Lyα and the Mg II index and also a more realistic two-component representation of Lyα that separates the long- and short-term variability (Worden et al. 1996). The latter uses the 81 day average of Mg II to estimate the long-term variation and the difference between Mg II and the 81 day average for the rotational modulation and short-term variations in general. The relations between the Lyα irradiance in units of photons $cm^{-2} s^{-1}$ and the Mg II index are

$$Ly\alpha_{SOLSTICE} = (-3.56 \times 10^{12}) + (1.479 \times 10^{13} Mg\ II) , \quad (1)$$

$$Ly\alpha_{SOLSTICE} = (-3.807 \times 10^{12}) + (1.570 \times 10^{13} Mg\ II_{81})$$
$$+ [0.922 \times 10^{13} (Mg\ II - Mg\ II_{81})] , \quad (2)$$

$$Ly\alpha_{SME} = (-1.757 \times 10^{12}) + (0.762 \times 10^{13} Mg\ II) , \quad (3)$$

$$Ly\alpha_{SME} = (-1.797 \times 10^{12}) + (0.778 \times 10^{13} Mg\ II_{81})$$
$$+ [0.648 \times 10^{13} (Mg\ II - Mg\ II_{81})] . \quad (4)$$

The linear relations given in equations (1) and (3) are analogous to the one derived by Lean (1990) for *SME* Lyα and helium data. The relations including both the long- and short-term variations in equations (2) and (4) are based on the same computational scheme used by Worden et al. (1996), but the coefficients used here are slightly different because they are derived from a longer set of data. The two resulting time series for the inferred Lyα values are shown in the bottom panel of Figure 3. Lyα values derived from SOLSTICE are higher and have a higher minimum-to-maximum variation.

Both *SME* and SOLSTICE measurements refer to the integrated line irradiance, while the *Voyager* IP Lyα glow depends only on the flux at the line center. This is because only the central core of the solar H Lyα line is scattered by the interplanetary hydrogen. Although the scattered wavelength can shift slightly with radial velocity, it is always within 0.01 nm of the line center. At present, it is not established that the temporal variations of the H Lyα core and the total intensity are the same throughout the solar cycle and, if so, whether their ratio is simply unity. Very few high-resolution observations of the solar Lyα line have been made. Simultaneous measurements of the total and central solar Lyα were made with *OSO 5* during the years 1969–1972 and in 1974, and the two periods gave contradictory results for the relationship between the integrated line and the core (Vidal-Madjar 1975; Vidal-Madjar & Phissamay 1980). Lyα profiles with high spatial and spectral resolution were also made by the ultraviolet polarimeter on the *Solar Maximum Mission* satellite (Fontenla, Reuchmann, &

Tandberg-Hanssen 1988). They showed clearly that different line profiles correspond to different regions of the solar atmosphere (quiet regions, active network, and sunspots). However, a careful analysis of the variability for the full-disk, average Lyα profile has never been published. This information would greatly improve the study of the IP Lyα variability in relation to solar measurements.

Another difficulty in comparing *Voyager* IP Lyα observations with solar observations made near the Earth is the position of the spacecraft and their different perspectives of the Sun. Not only are the two *Voyagers* many AU from the Sun, but their trajectories lie outside the ecliptic plane. This different geometry implies that for a certain day the two *Voyager* spacecraft see a face of the Sun that differs from the one seen simultaneously at Earth. Therefore, to estimate the solar flux at the time of the *Voyager* observations, some approximations are necessary. We find the 2 days within one solar rotation period when the Earth was at the solar longitude of the *Voyager* at the time of the measurement and compute a weighted average of the solar Lyα flux on these 2 days, but we neglect the latitudinal differences. The solar fluxes computed in this way (subspacecraft solar fluxes) can be compared with the *Voyager* data after they have been corrected for the spatial variations that arise from the heliocentric distance and the scattering of solar Lyα by the IP medium, which are evaluated using the model of Quémerais & Bertaux (1993). This is a first approach that neglects the fact that at large distances from the Sun, the IP Lyα intensity is related not only to the solar intensity in the direction defined by the Sun and the spacecraft but also to a contribution from photons coming from different directions and scattered in the interplanetary medium. In a second approach, we have used the model of Quémerais et al. (1993) that computes Lyα interplanetary intensities taking into account effects of multiple scattering combined with a nonuniform solar Lyα flux from the Sun. In this study, only variations of the solar flux in heliographic longitude are considered, although some variations in heliographic latitude may be found as well (Pryor et al. 1996).

Both of these approaches have been used in this work. The solar subspacecraft flux provides a straightforward way to represent the solar temporal variability reflected in the IP Lyα emission as a time series that clearly shows the 11 year solar cycle signature (Figs. 7–9); the second approach gives a more rigorous way to compare data and models, and we have used it to define the best fit between models and data or to derive correlations between them (Figs. 10 and 11).

While solar observations from Earth refer to the solar equator (except for a 7° inclination to the ecliptic), *Voyager* observations can be in any direction. Even if *Voyager* were at the solar longitude of Earth, the line of sight can extend over a range of ecliptic latitudes. Latitudinal differences are probably not very significant at solar minimum, when only few active regions are visible on the solar disk but become more important at solar maximum when the polar regions of the Sun are less active than the equatorial ones (Pryor et al. 1996), and latitudinal variations should be included in a model computation. However, at the distances of the *Voyager* spacecraft, this effect is moderated by the large optical thickness of the IP medium. Multiple scattering computations show that the rotational modulation, caused by an inhomogeneous distribution of active regions on the solar surface, is significantly damped after 10 AU (Quémerais et al. 1996). Analogously, latitudinal differences

in the solar flux are reduced as well. In this work we have not considered measurements within 15° of the ecliptic poles, where the latitudinal effect is most pronounced, and we have assumed that, in first approximation, the effect of latitudinal variations for the remaining *Voyager* data is negligible. The latitudinal effect could be taken into account using the technique developed by Pryor et al. (1996) to estimate solar Lyα irradiance through the He 1083 nm synoptic maps. This method depends on using the He 1083 nm index, as these are the only data with a long coverage in time and latitudinal information. Unfortunately, the Mg II index, which is a better proxy and follows Lyα variations more closely, is not available from solar images.

4. DESCRIPTION OF THE MODELS

The models of the interplanetary hydrogen distribution used in this study have been described by Lallement, Bertaux, & Dalandier (1985) and are equivalent to the model developed by Thomas (1978). They correspond to what is often called the standard hot model. The interstellar hydrogen distribution is represented by a Gaussian distribution characterized by a bulk velocity, V_0, equal to 20 km s^{-1} and a thermal velocity spread corresponding to a temperature, T_0, of 8000 K. These parameters have been determined by Bertaux et al. (1985). The hydrogen density in the interstellar medium, N_H, is taken in the range 0.1–0.2 cm^{-3}, which corresponds to the various estimates obtained by different studies (Shemansky et al. 1984; Ajello et al. 1993; Quémerais et al. 1994). In the vicinity of the Sun, the combined effects of radiation pressure and solar gravitational attraction result in a central force varying as the inverse of the square of the distance to the Sun. This force may be attractive or repulsive according to the value of the solar Lyα irradiance. It can be represented by the parameter μ, the ratio of the radiation pressure force to the gravitational force. When this value is smaller than unity, i.e., when the solar Lyα line-center flux at 1 AU is smaller than 3.3×10^{11} photon cm^{-2} s^{-1}, the net force is attractive, which means that hydrogen atoms get closer to the Sun than when μ is larger than unity. For this reason, μ is often called the focusing parameter.

The second solar parameter affecting the hydrogen distribution near the Sun is the neutral hydrogen lifetime at 1 AU, noted T_d. Interplanetary hydrogen atoms are ionized by two main sources. The most important ($\approx 80\%$) is charge exchange with solar wind protons. In the first approximation, its rate, β_{ex}, is equal to the product of the charge exchange cross section, σ_{ex}, and the solar wind proton flux. The second source of ionization of neutral hydrogen is photoionization by EUV solar photons with wavelengths below 91.2 nm. The combined ionization rates vary as the inverse of the square of the distance to the Sun, so the total ionization can be characterized by its rate at 1 AU or by the reciprocal of this rate, which is called the hydrogen lifetime at 1 AU. This parameter varies during the solar cycle with a mean value around 1.2×10^6 s. It can be determined from the solar wind proton flux measurements obtained by the *Interplanetary Monitoring Platform 8* (*IMP 8*) satellite. These data are available from the National Space Science Data Center (NSSDC) database (Pryor et al. 1992; Quémerais et al. 1994). The main effect of ionization is to create a region surrounding the Sun devoid of neutral hydrogen atoms. This region is elongated in the downwind direction and is called the ionization cavity. The size of this

cavity gives a measurement of the total ionization rate and so of the total solar wind proton flux (Bertaux et al. 1995).

Our models are time stationary and do not include effects of variation of the solar parameters during the solar cycle. As shown by Kyrölä, Summanen, & Raback (1994) and Ruciński & Bzowski (1995), this effect can be significant near the Sun. In the present study, the heliocentric distances of the *Voyager* spacecraft are rather large (always more than 5 AU), and we approximate the solar cycle variation by interpolating various models computed for different values of the neutral H lifetime parameter, T_d. The relevant value of T_d for each data point is obtained by averaging daily *IMP 8* data over the 1 year period preceding the measurement (Quémerais et al. 1994) to account for the travel time of hydrogen atoms across the ionization cavity. At large distances from the Sun, this provides a correct representation of the effects of the variation of the ionization rate during the solar cycle.

We have used the numerical scheme developed by Quémerais & Bertaux (1993) to compute the interplanetary Lyα glow pattern for a given neutral hydrogen distribution in the interplanetary medium. This scheme assumes that the multiple scattering effects are correctly represented by applying the complete frequency redistribution approximation to an isothermal gas having a temperature, T_0, and a constant bulk velocity, V_0, relative to the Sun. The spectral shape of the illuminating solar Lyα flux is assumed constant, i.e., possible variations of flux within 0.02 nm of the line center are neglected. The Lyα scattering phase function is applied to the first order of scattering. Finally, variations of the solar Lyα flux in heliographic longitude are taken into account. This last part of the modeling and its application to the study of the solar rotational modulations of the *Voyager* UVS Lyα data has been described by Quémerais, Sandel, & de Toma (1996).

We have seen that the models used here are characterized by two solar parameters, μ and T_d, and by three interstellar parameters, N_H, V_0, and T_0. The last two parameters are rather well constrained, and we will assume the values quoted above. The two solar parameters vary with the solar cycle, whereas N_H is constant but is not well constrained, and we need to investigate various possible values.

The radiation pressure parameter is directly proportional to the solar Lyα line-center intensity. Because there are very few measurements of the solar Lyα spectral shape integrated on the solar disk (Lemaire et al. 1978), a relationship between the line-center flux and the integrated line flux must be used to estimate the effective flux relevant to the study of interplanetary hydrogen. A simple step is to assume that this relationship is constant during the solar cycle. From the few previous measurements, it was found that the integrated line flux is approximately equal to the line-center flux multiplied by an equivalent width of 1 Å (Vidal-Madjar 1975; Lemaire et al. 1978). As a consequence, the parameter μ can then be determined by direct measurements of the solar Lyα integrated flux. In this work we have used data from *SME* and SOLSTICE. When the time of our observations does not correspond to an existing measurement, we have used indices of solar activity to infer the values of solar Lyα, as described in the previous section. Using the *SME* values and averaging over a 1 year period prior to the measurement, the resulting μ varies between 0.7 and 1.2. The same estimate from the SOLSTICE data set yields values of μ between 1 and 1.8, which means that

radiation pressure is always dominant and that there is no focusing on the downwind axis, thus leading to a much larger ionization cavity in the downwind direction. Fortunately, because the *Voyager* spacecraft are moving toward the upwind direction, this uncertainty is not so important for our data set after 1980. To evaluate this effect, we have made several model computations with different values of μ. In Figure 4, we show a comparison of model results for three different sets of parameters. Each point corresponds to the line of sight of an actual measurement made by *Voyager 2*.

We choose a model computation characterized by $T_d = 1.2 \times 10^6$ s, $\mu = 1$, and $N_H = 0.15$ cm^{-3} as a reference model. The range of variations from this reference model for different values of μ is then given by the two plots in Figure 4. The top curve corresponds to the ratio of a model with $T_d = 1.2 \times 10^6$ s, $N_H = 0.15$ cm^{-3}, and $\mu = 0.7$ with the reference model. The bottom curve is for the same parameters except that μ is equal to 1.5. We see that after 1982, most of the points are affected slightly (within 5%) by a change in the radiation pressure. At large distances from the Sun, only measurements having the line of sight near the Sun are affected by the uncertainty in μ. We have made a similar study for the sensitivity to T_d. Here, the estimates obtained from the *IMP 8* data set available from the NSSDC show that T_d varies between 1.0×10^6 and 1.5×10^6 s. In Figure 5, we show the same type of comparison as in Figure 4 with the reference model with $T_d = 1.2 \times 10^6$ s, $N_H = 0.15$ cm^{-3}, and $\mu = 1$. The top curve shows the ratio obtained for *Voyager 1* and a model with a lifetime of 1.5×10^6 s. The bottom curve is for a ratio with a lifetime of 1.0×10^6 s. The range of variation is larger than in the previous case, but here again, the different models have the same limit far away from the Sun because the solar parameters have a strong signature only close to the Sun.
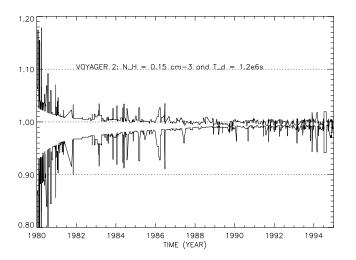

FIG. 5.—Calculation of model sensitivity to the neutral H lifetime at 1 AU, T_d. The top curve corresponds to the ratio of a model defined by $\mu = 1$, $N_H = 0.15$ cm^{-3}, and $T_d = 1.5 \times 10^6$ s to the reference models defined by $\mu = 1$, $N_H = 0.15$ cm^{-3}, and $T_d = 1.2 \times 10^6$ s. The bottom curve is for the ratio of a model with $\mu = 1$, $N_H = 0.15$ cm^{-3}, and $T_d = 1.0 \times 10^6$ s to the reference model. The sensitivity observed here is larger than for the μ parameter. A similar result is obtained for *Voyager 1*.

Finally, since N_H is not accurately known within the range 0.1–0.2 cm^{-3}, we have evaluated the effect of this parameter on our model computations. We have used the same reference model as before and fixed the values of the solar parameters. When N_H is different, the models do not have the same limit at large distances from the Sun. So, the models have been scaled arbitrarily to the average value of the ratio in 1995. The top curve in Figure 6 corresponds to the ratio between $N_H = 0.2$ cm^{-3} and the reference model, whereas the bottom curve corresponds to the ratio between the model with $N_H = 0.1$ cm^{-3} and the reference model. Changing the value of N_H affects the mean slope of the decrease in Lyα flux with distance. In particular, because the extinction effects are larger with increasing optical thick-

FIG. 4.—Calculation of model sensitivity to the radiation pressure parameter, μ, in the case of the *Voyager 2* data set. To illustrate this effect, we have compared the background intensities corresponding to the *Voyager 2* observations computed with different values of μ. In the plot, the ratio of IP Lyα model computations in two cases is shown as a function of time. The top curve corresponds to the ratio of a model with $\mu = 0.7$ to a model with $\mu = 1$. The bottom curve shows the ratio of a model with $\mu = 1.5$ to the reference case with $\mu = 1$. In each case, $T_d = 1.2 \times 10^6$ s and $N_H = 0.15$ cm^{-3}. As time increases, the distance between the Sun and the spacecraft increases. Then, effects of the variation of the solar radiation pressure become less important. A similar result, not shown here, is obtained with *Voyager 1*.
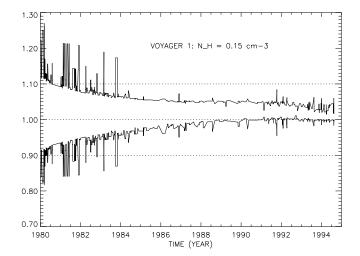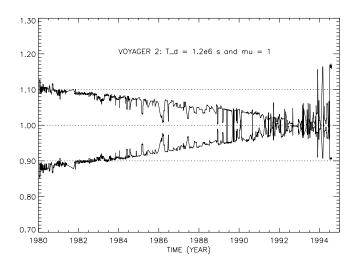

FIG. 6.—Calculation of model sensitivity to the neutral hydrogen density of the interstellar medium, N_H. A model defined by $\mu = 1$, $T_d = 1.2 \times 10^6$ s, and $N_H = 0.15$ cm^{-3} is used as a reference. The top curve corresponds to the ratio of a model with $\mu = 1$, $T_d = 1.2 \times 10^6$ s, and $N_H = 0.2$ cm^{-3} to the reference model. The bottom curve corresponds to the ratio of a model with $\mu = 1$, $T_d = 1.2 \times 10^6$ s, and $N_H = 0.1$ cm^{-3} to the same reference model. The two curves are arbitrarily scaled to a mean value of 1 in 1994. A similar result is obtained for *Voyager 1*.

ness, we see that the case with $N_H = 0.2$ cm^{-3} decreases faster than the other two cases. The large oscillations in Figure 6 during the last years correspond to changes in the line of sight. They are caused by the anisotropy of the IP Lyα glow, which is brighter in the solar direction and dimmer in the antisolar direction. The IP Lyα anisotropy is affected by the hydrogen number density, N_H, assumed in the model especially at large distances from the Sun. As the opacity of the IP medium increases, the radiative transfer effects grow. For a given position from the Sun, a larger hydrogen number density leads to a larger opacity at Lyα. This tends to decrease the Lyα background anisotropy caused by the hydrogen ionization cavity around the Sun. As appears in Figure 6, changing the N_H parameter has quantitatively different effects for lines of sight near the Sun and close to the antisolar direction.

The three main model parameters affect the interpretation of the *Voyager* data sets in different ways. The two solar parameters, T and μ, become less important as the distance between the Sun and the spacecraft increases. After 1982, most of the points are affected very little by the variability in radiation pressure. The effect is more important for the H lifetime parameter. To minimize uncertainty from this source, we have used the values of T_d computed from the *IMP 8* proton flux measurements at Earth orbit. The models for various values of T_d were interpolated according to the value obtained by averaging the *IMP 8* flux measurements over a 1 year period. Finally, we have shown that N_H is more important at large distances from the Sun. It defines the mean slope of the decreasing backscattered Lyα intensity as a function of time or increasing solar distance.

5. RESULTS

The two IP Lyα data sets obtained from the *Voyager* spacecraft are shown in Figure 7. The two time series are in good agreement after 1982 and show a clear signature of the 11 year solar cycle reflected in the *Voyager* IP Lyα fluxes. During the first 2 years, the data from *Voyager 1* and
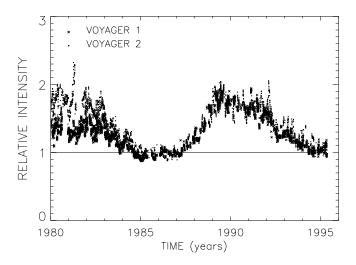
FIG. 7.—*Voyager 1* and *Voyager 2* IP Lyα measurements as a function of time. The data have been divided by a model with a constant solar flux to account for the differences due to the position of the spacecraft. The model selected has $\mu = 1$, $N_H = 0.15$ cm^{-3}, and an interpolated T_d. The data are normalized to an average minimum value based on observations in 1986, during solar minimum for solar cycle 21. A clear 11 year solar cycle signature is present in the data. The measurements from the two spacecraft are in general good agreement after 1982. The difference of about 30% in the first 2 years is not completely understood.

Voyager 2 show some differences. Even given that a direct comparison is not possible because the two spacecraft do not have daily observations and were observing the Sun from different positions, a general difference in level of about 30% is clearly present. With the model used, the data obtained with *Voyager 1* during the years 1980–1981, which correspond to solar maximum in solar cycle 21, appear underestimated relative to the data in 1989–1991, which correspond to the maximum in solar cycle 22. This result is model dependent. As seen in the previous section, using different input parameters can give quite different results in the model computation, especially during the first years, when the spacecraft were closer to the Sun. If a different model is used, the values of the two solar maxima will change accordingly in intensity, which gives a different time series for each spacecraft. For example, if we use a model with a very low value for T_d, e.g., 1.0×10^6 s., the two maxima in the *Voyager 1* data will have about the same level, but the first maximum in the *Voyager 2* data will be very enhanced compared to the later one. We tried several different sets of parameters, but we did not find models that could eliminate the difference between the two data sets, and some discrepancy was always present during the first 2 or 3 years of data. On the other hand, it is difficult to explain a difference of this level between the two spacecraft in terms of changes in the instrument sensitivity because the two *Voyager* UVS have been very stable after the encounter with Jupiter in 1979; yet, because the central Lyα channels cannot be directly monitored with repeated stellar observations, it is possible that some undetected changes in the instrument contributed to the difference seen. At present, the disagreement between the two *Voyager* spacecraft during the first years remains unexplained and seems to suggest that a more complex model may be needed in the vicinity of the Sun.

In Figure 8 we compare the same *Voyager 1* and *Voyager 2* data shown in Figure 7 with SOLSTICE solar subspacecraft fluxes. An estimated solar subspacecraft flux, which is based on a linear relationship with the Mg index that includes the long-term and the rotational modulation (eq. [2]), is also shown. A linear, 1:1 ratio between Lyα core and the integrated line irradiances is assumed in the comparison. We notice that *Voyager 2* data are in extremely good agreement with the subspacecraft fluxes predicted from the SOLSTICE-Mg II index relation and that *Voyager 1* data are also in good agreement after 1985. During the years 1992–1995 of the *UARS* mission, both spacecraft agree very well with SOLSTICE solar data. The same comparison, but for *SME* solar subspacecraft data and estimated irradiances (eq. [4]), is shown in Figure 9. The variability during the solar cycle seen in *SME* data disagrees with that of the *Voyager* data, which have a larger variation. *Voyager 2* data in relation to *SME* data seem to suggest that a nonlinear relationship between the Lyα core and the integrated line may be appropriate or that the *SME* instrument calibration is not well understood over the long term.

We made comparisons analogous to the one just described for several models. Here we present the results obtained with nine different sets of values for the three parameters discussed in the previous section. For T_d we used values of 1.0×10^6, 1.2×10^6, and 1.5×10^6 s as well as the interpolated values of T_d. For N_H we selected the two values 0.10 and 0.15 cm^{-3}. The parameter μ is not well
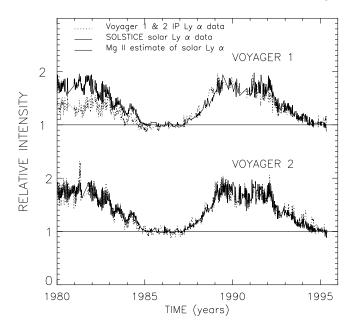
FIG. 8.—Comparison of the *Voyager 1* and *Voyager 2* IP Lyα measurements with subspacecraft fluxes based on SOLSTICE solar Lyα measurements. For times when SOLSTICE data are not available, the solar Lyα irradiance is estimated by a linear relationship with the Mg II index that accounts for the short- and long-term variability. The same model used in Fig. 7 is used here to correct the data for spatial effects. The data have been divided by an average solar minimum value.

FIG. 9.—The same as Fig. 8 but for *SME* solar Lyα measurements

known, but unfortunately we do not know the absolute calibration of the *Voyager* UVS well enough to determine the absolute intensity of IP Lyα emission. Besides, *Voyager* data, because of the large distance from the Sun of the two spacecraft and their position relative to the interstellar hydrogen flux, are not very appropriate for determining the best value for μ. Therefore, we eliminated from the *Voyager* data set all the points for which a model with $\mu = 0.7$ or 1.5 differs by more than 5% from the model with the same parameters, but $\mu = 1$. This condition eliminates almost all
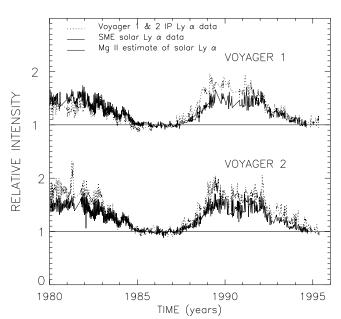
the observations before 1982, i.e., closer to the Sun, and a few more, later points where the pointing direction is toward the downwind cavity. The number of observations remaining are 1982 for *Voyager 1* and 2785 for *Voyager 2*, which still gives good statistics and time coverage. This selection allowed us to use a value of $\mu = 1$ for all the models and to study the other parameters. All the models were tested against *Voyager 1* and *Voyager 2* data using both *SME* and SOLSTICE solar data as input.

The results of the study between *Voyager* data and solar subspacecraft fluxes are summarized in Tables 2 and 3. Eight different models with $\mu = 1$ are considered. A case with $\mu = 1.5$, which would be more consistent with SOLSTICE Lyα absolute irradiances, is added for completeness. Both SOLSTICE and *SME* data and their relationship with

TABLE 2

Voyager 1 Data/Constant Model: Solar Subspacecraft Values

Model	Mg-SOLSTICE	Mg-*SME*	He-SOLSTICE	He-*SME*	SOLSTICE	*SME*
Number of points	2303	2195	2303	2195	509	1253
	1779	1701	1779	1701	507	1160
$\mu = 1.0, N_H = 0.15, T_d$ interpolated	11.068	10.316	10.347	10.644	7.222	10.111
	8.587	9.510	9.796	10.657	7.236	10.176
$\mu = 1.0, N_H = 0.10, T_d$ interpolated	8.736	8.788	8.349	9.347	7.644	9.179
	7.710	9.019	8.565	9.837	7.638	9.192
$\mu = 1.5, N_H = 0.15, T_d$ interpolated	9.597	9.920	10.082	10.955	7.953	9.836
	8.533	9.608	9.853	10.806	7.959	10.054
$\mu = 1.0, N_H = 0.15, T_d = 1.5E6$	11.745	11.148	11.483	11.804	8.313	11.304
	9.921	10.618	11.174	11.893	8.323	11.029
$\mu = 1.0, N_H = 0.10, T_d = 1.5E6$	9.576	9.678	9.714	10.620	8.726	10.399
	8.675	9.657	9.680	10.752	8.698	9.956
$\mu = 1.0, N_H = 0.15, T_d = 1.2E6$	9.638	9.714	9.978	10.764	7.237	10.350
	8.995	9.928	10.273	11.183	7.251	10.519
$\mu = 1.0, N_H = 0.10, T_d = 1.2E6$	8.171	9.270	9.282	10.674	7.983	9.186
	7.998	9.148	8.864	10.101	7.979	9.243
$\mu = 1.0, N_H = 0.15, T_d = 1.0E6$	8.167	9.257	9.515	10.785	7.450	9.137
	7.623	8.686	8.784	9.842	7.459	9.342
$\mu = 1.0, N_H = 0.10, T_d = 1.0E6$	8.738	10.715	10.785	12.420	7.842	8.648
	7.565	8.887	8.278	9.662	7.851	8.642

NOTE.—Root mean squared (rms) values, in percent, between the *Voyager 1* data shown in Figs. 9 and 10 and models for nine different models. The number of observations used for the computation of the rms values is given in the first row. For each model, the top value refer to all data available; the second one, to the subset of points that are not strongly affected by μ.

TABLE 3

Voyager 2 Data/Constant Model: Solar Subspacecraft Values

Model	Mg–SOLSTICE	Mg–*SME*	He–SOLSTICE	He–*SME*	SOLSTICE	*SME*
Number of points	3249	3159	3249	3159	632	1603
	2615	2546	2615	2546	581	1491
$\mu = 1.0$, $N_H = 0.15$, T_d interpolated	6.090	8.129	7.870	9.326	6.489	8.838
	5.436	7.867	6.931	8.645	5.358	8.805
$\mu = 1.0$, $N_H = 0.10$, T_d interpolated	7.313	10.099	9.431	11.290	6.535	9.620
	6.723	8.981	7.705	9.535	6.776	9.415
$\mu = 1.5$, $N_H = 0.15$, T_d interpolated	8.388	10.863	10.921	12.449	7.613	8.691
	5.354	8.038	7.093	8.927	5.451	8.812
$\mu = 1.0$, $N_H = 0.15$, $T_d = 1.5E6$	6.684	9.239	9.175	10.768	6.006	9.234
	6.139	8.638	8.094	9.776	5.424	9.137
$\mu = 1.0$, $N_H = 0.10$, $T_d = 1.5E6$	7.974	11.055	10.652	12.557	6.925	9.795
	6.668	9.104	8.237	10.087	7.013	9.454
$\mu = 1.0$, $N_H = 0.15$, $T_d = 1.2E6$	7.434	10.290	10.274	11.944	6.596	8.972
	5.672	8.356	7.559	9.369	5.460	9.019
$\mu = 1.0$, $N_H = 0.10$, $T_d = 1.2E6$	9.757	12.846	12.579	14.432	6.529	9.536
	6.781	9.170	8.025	9.916	6.779	9.467
$\mu = 1.0$, $N_H = 0.15$, $T_d = 1.0E6$	9.915	12.702	12.743	14.361	7.569	8.858
	5.436	8.153	6.916	8.857	5.370	9.026
$\mu = 1.0$, $N_H = 0.10$, $T_d = 1.0E6$	12.619	15.574	15.431	17.187	6.474	9.655
	7.397	9.651	8.257	10.123	6.622	9.788

Note.—Rms values, in percent, for *Voyager 2* data. The format is the same as in Table 2.

Mg II and He 1083 nm indices are used to derive sub-spacecraft fluxes. The root mean square (rms) deviation is used to evaluate the quality of the fit between data and models. The first number listed for each model gives the rms value using all available data; the second number is the rms value based only on the subset of data that is insensitive to a change in the value of μ.

For *Voyager 1*, if we discard the models with $T_d = 1.0 \times 10^6$ s, which do not seem to be supported by the *IMP 8* observations, the best fit over the entire period is obtained with solar fluxes derived from SOLSTICE data and Mg II index and a model with $\mu = 1$, $N_H = 0.10$ cm^{-3}, and $T_d = 1.2 \times 10^6$ s. Also, a model with $\mu = 1$, $N_H = 0.10$ cm^{-3}, and an interpolated value for T_d gives a good fit. For both models, the correlation coefficient between *Voyager* data and subspacecraft solar fluxes is $r = 0.913$. The good fits obtained for *Voyager 1* data with a value of $T_d = 1.0 \times 10^6$ s and/or $N_H = 0.10$ cm^{-3} seem to be related to the differences between the two maxima in *Voyager 1* time series, because, as shown in Figures 5 and 6, both cases predict lower values for the IP Lyα during the first years. When we consider the fits with real solar measurements, the best fit is for SOLSTICE Lyα data and a model with $\mu = 1$, $N_H = 0.15$ cm^{-3}, and interpolated value for T_d, which is consistent with the results of the *Voyager 2* data analysis. For *Voyager 2*, the best fit is obtained with solar fluxes derived from SOLSTICE and Mg index and a model with $\mu = 1$, $N_H = 0.15$ cm^{-3}, and interpolated value for T_d. The correlation found in this case is $r = 0.960$. We notice that solar subspacecraft fluxes based on the helium index have higher rms values and slightly lower correlations than those based on the magnesium index, but there is general good agreement between them. Also, *Voyager 1* data usually have higher rms values than *Voyager 2* and lower correlations.

Assuming a linear relation between the integrated Lyα and the Lyα core irradiances, SOLSTICE data always have smaller rms values and higher correlations than *SME* data. *SME* solar data in comparison with *Voyager 2* data suggest that a nonlinear relation between the integrated Lyα and the Lyα core irradiances may give a better fit than a linear one. All nine models for both spacecraft have been tested against the nonlinear relation between the integrated Lyα and the Lyα core irradiance given by Vidal-Madjar (1975), based on *OSO 5* data:

$$\mathrm{Ly}\alpha_{\mathrm{core}} = 0.54 \times \mathrm{Ly}\alpha_{\mathrm{line}}^{1.53} , \qquad (5)$$

where Lyα$_{\mathrm{core}}$ is in units of photons cm^{-2} s^{-1} Å^{-1}, and Lyα$_{\mathrm{line}}$ is in units of photons cm^{-2} s^{-1}. This relationship increases the amplitude of the variation for Lyα core by about 50%. When equation (5) was used, the rms values found for *Voyager 1* were worse for all cases. Ratios of data to models with subspacecraft fluxes based on SOLSTICE data or derived from indices and SOLSTICE had rms values 4%–7% higher, while for *SME* or *SME*-derived subspacecraft solar fluxes, rms values were only 0.2%–2.5% higher. For *Voyager 2*, ratios of data to models with subspacecraft solar fluxes based on SOLSTICE were found again to have rms values 4%–7% worse, while subspacecraft solar fluxes based on *SME* had 0.5%–2% lower rms values. In all cases, the smaller rms values found between *Voyager 2* and *SME* data using equation (5) were still higher by about 1% than the rms values for the same models but with a linear relation and SOLSTICE data. On the basis of this study, we conclude that a nonlinear relation between integrated Lyα and Lyα core irradiances, like the one suggested by Vidal-Madjar, does not improve the fit with the *Voyager* data and seems to overestimate the long-term variation of the scattered Lyα.

In the analysis just described, the *Voyager* IP Lyα data were represented as a time series analogous to solar Lyα data that very clearly shows the 11 year solar cycle. A different and more accurate comparison of *Voyager* data with model predictions can be made using a radiative transfer computation that takes into account the effect of multiple scattering. The results of this analysis are summarized in Table 4, and the ratios between observed and computed fluxes are shown in Figures 10 and 11. In this study we use mainly the observations not affected by variability in the radiation pressure parameters by more than 10%, which give the best way of evaluating the other parameters. Only solar irradiances derived from *SME* and SOLSTICE relationships with the Mg index are used. Irradiances

TABLE 4

Voyager 1 AND 2 Data: Model with Multiple Scattering

MODEL	Voyager 1		Voyager 2	
	Mg-SOLSTICE	Mg-*SME*	Mg-SOL	Mg-*SME*
Number of points	2310	2310	3275	3275
	1786	1786	3153	3153
$\mu = 1.0$, $N_H = 0.15$, T_d interpolated......	10.306	9.832	5.854	8.027
	8.033	9.016	5.297	7.715
$\mu = 1.0$, $N_H = 0.10$, T_d interpolated......	8.022	8.264	7.383	9.999
	7.159	8.488	6.609	8.780
$\mu = 1.5$, $N_H = 0.15$, T_d interpolated......	8.982	9.470	8.434	10.777
	7.981	9.094	5.262	7.896
$\mu = 1.0$, $N_H = 0.15$, $T_d = 1.5E6$	11.058	10.706	6.638	9.210
	9.417	10.170	6.026	8.535
$\mu = 1.0$, $N_H = 0.10$, $T_d = 1.5E6$	8.935	9.205	8.161	11.022
	8.123	9.139	6.560	8.955
$\mu = 1.0$, $N_H = 0.15$, $T_d = 1.2E6$	8.985	9.259	7.561	10.271
	8.468	9.448	5.593	8.237
$\mu = 1.0$, $N_H = 0.10$, $T_d = 1.2E6$	7.685	8.846	10.034	12.803
	7.425	8.607	6.683	8.993
$\mu = 1.0$, $N_H = 0.15$, $T_d = 1.0E6$	7.657	8.852	10.151	12.671
	6.994	8.139	5.369	7.991
$\mu = 1.0$, $N_H = 0.10$, $T_d = 1.0E6$	8.551	10.412	12.950	15.523
	7.001	8.341	7.332	9.453

NOTE.—Rms values, in percent, for the *Voyager 1* and 2 data and a radiative transfer model computation.

derived from the He 1083 nm index are not included because they agree with those computed from the Mg II index but have lower correlation, and they do not add any further information to the fittings. A simple linear relationship between Lyα and the Mg II index (eqs. [1] and [3]) can be used because multiple scattering reduces the effect of the rotational modulation.

We notice that the rms values are usually lower than in the previous comparison, which confirms that the results of a radiative model computation represent the data better than do the subspacecraft fluxes. A model with interpolated T_d and density at infinity of 0.10–0.15 cm^{-3} gives a good fit

for both *Voyager 1* and *Voyager 2* data sets. Also, a model with $T_d = 1.0 \times 10^6$ s and $N_H = 0.15$ cm^{-3} gives a good fit but does not seem consistent with *IMP 8* measurements.

Voyager Lyα observations are particularly valuable for the period 1989–1991, when no direct measurements of the solar Lyα irradiance were available. During this time *Voyager* measurements correlate well with the He 1083 nm and the Mg II indices as shown in Figure 8. Another estimate of the variation in the EUV solar irradiance during this period is available from the *Pioneer Venus* Langmuir probe. The photoelectron current I_{pe} emitted from the probe depends on the solar irradiance in the band 10–130 nm; Lyα contributes about 56% of the total current (Hoegy et al. 1993). In Figure 12 we compare our estimate of the variation in solar H Lyα with the 81 day average of I_{pe} from
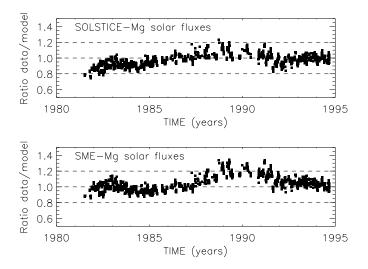
FIG. 10.—Representation of the data-to-model ratio for *Voyager 1* as a function of time. There are 1982 individual measurements. The observations affected by the variability of radiation pressure have been eliminated in this plot. The variation of the ionization rate during the solar cycle has been taken into account. The radiation pressure and density parameters are $\mu = 1$ and $N_H = 0.15$ cm^{-3}. The graph in the top panel corresponds to an estimate of the illuminating flux obtained from magnesium data correlated to the SOLSTICE values for the solar Lyα irradiance, and the bottom panel corresponds to the correlation with the *SME* values.
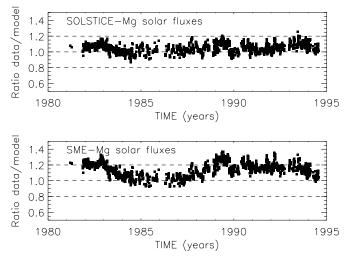
FIG. 11.—Representation of the data-to-model ratio for *Voyager 2* as a function of time. There are 2785 individual measurements. The models are the same as in the previous figure. Here, for *Voyager 2* and using the SOLSTICE flux estimate, the data-to-model ratio stays within 12% of the average value. This means that, within that accuracy, the relationship between the integrated solar Lyα line and the flux at line center remains constant during the solar cycle.
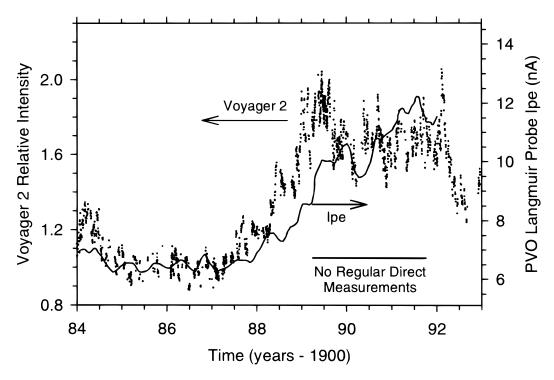
Fig. 12.—Comparison of our estimate of the variation in solar H Lyα flux from *Voyager 2* (Fig. 8) with the 81 day average of I_{pe} derived from the *Pioneer–Venus* Langmuir probe (Hoegy et al. 1993). The scales have been chosen so that the two indices match near solar minimum and so that the suppressed zeros coincide. The *Voyager* measurements indicate a more rapid rise in 1989, followed by a decrease in 1990–1991, when I_{pe} was still increasing.

Hoegy et al. (1993). The shapes of the two estimates are quite different. The *Voyager 2* data show a more rapid increase during the rising phase of solar cycle 22, reaching higher values in 1989, compared to I_{pe}. The *Voyager* maximum values during 1991 are comparable to those in 1989 and not 20% higher as for the I_{pe} index, which, except for a decline in 1990, implies an almost linear increase during the years 1989–1991.

6. DISCUSSION

In the preceding section, we have shown that the variability of the solar Lyα irradiance measurements derived from the *UARS*/SOLSTICE data is in good agreement with the *Voyager* UVS Lyα background data. As explained before, our results are not accurate enough to estimate the absolute solar Lyα irradiance, but the importance of the discrepancy between the *SME* and SOLSTICE data must be pointed out. If the *UARS*/SOLSTICE solar irradiance measurements are correct, the radiation pressure is almost always stronger than gravitational attraction from the Sun. As a consequence, models predict a hydrogen ionization cavity that is much larger than measured, especially in the downwind region. In such a case, it is necessary to consider other effects that may fill the cavity in a consistent way. A first possibility is to increase our estimate of the temperature of the interstellar hydrogen penetrating the heliosphere. A second possibility is to decrease our estimate of the bulk velocity of the gas. Both possibilities have been considered, but they are in contradiction with previous measurements of these parameters obtained with the use of a hydrogen absorption cell (Bertaux et al. 1985) and other independent measurements obtained by Lallement, Bertaux, & Clarke (1993).

A third possibility is that the ratio between Lyα line core and integrated Lyα irradiances differs from unity, which allows lower values for the Lyα core to be consistent with *UARS*/SOLSTICE measurements. Previous measurements of the Lyα line shape by Lemaire et al. (1978) indicate that this ratio is close to 1 and seem to contradict this hypothesis, yet the high variability, both in the core and in the wings, of the Lyα line shown by Fontenla et al. (1988) in different regions on the solar disk suggest that an accurate relationship between Lyα line core and integrated Lyα irradiances is still not established.

Finally, as shown by Baranov & Malama (1993), the hydrogen velocity distribution should be affected strongly by the interface between the solar wind and the interstellar plasma at the heliopause. One effect would be the addition of a hot neutral component that may be relatively important near the Sun in the downwind region. This may also be responsible for a partial filling of the ionization cavity and thus allow for a larger absolute Lyα solar flux such as the one measured by SOLSTICE.

A change in the previously accepted values of solar Lyα irradiance and its variability over the solar cycle also affects previous studies of the hydrogen distribution in the interplanetary medium. The analysis of *Voyager 1*, *Voyager 2*, and *Pioneer 10* cruise maneuvers by Hall et al. (1993) relies on correction for temporal variations of the Lyα solar irradiances derived from the *SME* data set. The minimum-to-maximum ratio derived by *SME* solar measurements is lower than the one shown in SOLSTICE measurements. In such a case, it is likely that the quantitative conclusion drawn by Hall et al. (1993) should be revised, although the amplitude of the correction should not affect the qualitative conclusion that at large distances from the Sun, the anti-solar Lyα background intensity does not fall as quickly as predicted by models. This suggests that there is a secondary

component to the Lyα intensity that can be detected only at large distances from the Sun where the primary component has sufficiently decreased. It is too early in the observations to state if this second component is linked to an increase in hydrogen number density near the heliopause. A similar conclusion was drawn by Quémerais et al. (1995) using a different technique that is independent of temporal variations of the illuminating solar flux.

From Figures 10 and 11, it appears that the *UARS/ SOLSTICE* data set gives a better fit (mainly for *Voyager 2*). It is found that it is not necessary to use a nonconstant relationship between the Lyα line-center flux and the integrated line flux. However, because of the strong variations in line shape shown by Fontenla et al. (1988), it is unlikely that the global line shape is constant, and its variations may be responsible for some of the discrepancies we still find between the data and our models.

Anisotropies of the solar flux with heliographic latitude, which have not been taken into account here, are another source of error, although our preliminary estimates using the results of Pryor et al. (1996) have shown that the effect is very small for the data set used here.

The *Voyager* UVS IP Lyα data corresponding to the inner part of the heliosphere have been removed here because the corresponding models are very dependent on changes in radiation pressure. For these data it is necessary to use a time-dependent model as developed by Kyrölä et al. (1994) and Ruciński & Bzowski (1995) with the actual solar cycle variation of radiation pressure included.

REFERENCES

Ajello, J. M., Pryor, W. R., Barth, C. A., Hord, C. W., & Simmons, K. E. 1993, Adv. Space Res., 13(6), 37
Ajello, J. M., Pryor, W. R., Barth, C. A., Hord, C. W., Stewart, A. I. F., Simmons, K. E., & Hall, D. T. 1994, A&A, 289, 283
Ajello, J. M., Stewart, A. I. F., Thomas, G. E., & Graps, A. 1987, ApJ, 317, 964
Baranov, V. B., & Malama, Y. G. 1993, J. Geophys. Res., 98, 15,157
Bertaux, J. L., & Blamont, J. E. 1971, A&A, 11, 200
Bertaux, J. L., Lallement, R., Kurt, V. G., & Mironova, E. N. 1985, A&A, 150, 1
Bertaux, J. L., et al. 1995, Sol. Phys., 162, 403
Broadfoot, A. L., et al. 1977, Space Sci. Rev., 21, 183
Broadfoot, A. L., & Sandel, B. R. 1977, Appl. Opt., 16, 1533
Brueckner, G. E., Eldow, K. L., Floyd, L. E., Lean, J. L., & VanHoosier, M. E. 1993, J. Geophys. Res., 98, 10,695
Donnelly, R. F. 1991, J. Geomagn. Geoelectr., Suppl., 43, 835
Fontenla, J., Reichmann, E. J., & Tandberg-Hanssen, E. 1988, ApJ, 329, 464
Hall, D. T., Shemansky, D. E., Judge, D. L., Gangopadhyay, P., & Gruntman, M. A. 1993, J. Geophys. Res., 98, 15,185
Harvey, J. W. 1981, NASA Conf. Publ. 2191, 265
Harvey, K. L., Recely F., Hirman J., & Cohen, N. 1997, in Proc. Solar-Terrestrial Predictions Workshop, in press
Hoegy, W. R., Pesnell, W. D., Woods, T. N., & Rottman, G. J. 1993, Geophys. Res. Lett., 20, 1335
Holberg, J. B., & Watkins, R. 1992, *Voyager* Ultraviolet Spectrometer Guest Observer and Data Analysis Handbook, Lunar & Planet. Lab., Univ. Arizona
Keller, H. U., Richter, K., & Thomas, G. 1981, A&A, 102, 415
Kyrölä, E., Summanen, T., & Raback, P. 1994, A&A, 288, 299
Lallement, R., Bertaux, J. L., Chassefière, E., & Sandel, B. R. 1991, A&A, 252, 385
Lallement, R., Bertaux, J. L., & Clarke, J. T. 1993, Science, 260, 1095
Lallement, R., Bertaux, J. L., & Dalaudier, F. 1985, A&A, 150, 21
Lean, J. L. 1988, Adv. Space Res., 8(5), 263

Lean, J. L. 1990, J. Geophys. Res., 95, 11,933
Lemaire, P., Charra, J., Jouchoux, A., Vidal-Madjar, A., Artzner, G. E., Vial, J. C., Bonnet, R. M., & Skumanich, A. 1978, ApJ, 223, L55
Mount, G. H., & Rottman, G. J. 1983a, J. Geophys. Res., 88, 5403
———. 1983b, J. Geophys. Res., 88, 6807
———. 1985, J. Geophys. Res., 90, 13,031
Osterbart, R., & Fahr, H. J. 1992, A&A, 264, 260
Pryor, W. R., et al. 1992, ApJ, 394, 363
Pryor, W. R., et al. 1996, Geophys. Res. Lett., 23, 1893
Quémerais, E., & Bertaux, J. L. 1993, A&A, 277, 283
Quémerais, E., Bertaux, J. L., Sandel, B. R., & Lallement, R. 1994, A&A, 290, 941
Quémerais, E., Sandel, B. R., & de Toma, G. 1996, ApJ, 463, 349
Quémerais, E., Sandel, B. R., Lallement, R., & Bertaux, J. L. 1995, A&A, 299, 249
Rottman, G. J., Woods, T. N., & Sparn, T. P. 1993, J. Geophys. Res., 98, 10,667
Ruciński, D., & Bzowski, M. 1995, A&A, 296, 248
Shemansky, D. E., Judge, D. L., & Jessen, J. M. 1984, in IAU Coll. 81, Local Interstellar Medium (NASA Conf. Publ. 2345), ed. F. C. Bruhweiler, Y. Kondo, & B. D. Savage (Dordrecht: Reidel), 24
Thomas, G. E. 1978, Annu. Rev. Earth Planet. Sci., 6, 173
Thomas, G. E., & Krassa, R. F. 1971, ApJ, 134, 20
Vidal-Madjar, A. 1975, Sol. Phys., 40, 69
Vidal-Madjar, A., & Phissamay, B. 1980, Sol. Phys., 66, 259
White, O. R., Rottman, G. J., & Livingston, W. C. 1990, Geophys. Res. Lett., 17, 575
Woods, T. N., & Rottman, G. J. 1990, J. Geophys. Res., 95, 6227
———. 1997, J. Geophys. Res., 102, 8769
Woods, T. N., Rottman, G. J., & Ucker, G. J. 1993, J. Geophys. Res., 98, 10,679
Woods, T. N., et al. 1996, J. Geophys. Res., 101, 9541
Worden, J., Woods, T. N., Rottman, G. J., Schmidtke, G., Tai, H., & Doll, H. 1996, Opt. Eng., 35, 554